

**8<sup>th</sup> International Symposium on Negative Ions, Beams and Sources**  
**Orto Botanico, Padova, Italy**  
**2–7 October 2022**

## Correlation of H<sup>-</sup> beam properties to Cs-coverage

---

J. Lettry,<sup>a,\*</sup> A. Vnuchenko,<sup>a</sup> S. Bertolo,<sup>a</sup> C. Mastrostefano,<sup>a</sup> M. O'Neil,<sup>a</sup> F. di Lorenzo,<sup>a</sup>  
Y. Coutron,<sup>a</sup> D. Steyeart,<sup>a</sup> B. Riffaud,<sup>a</sup> J. Thiboud,<sup>a</sup> R. Guida,<sup>a</sup> K. Kapusniak,<sup>a</sup> C. Charvet,<sup>a</sup>  
B. Teissandier,<sup>a</sup> P. Moyret,<sup>a</sup> F. Roncarolo,<sup>a</sup> S. Bart Pedersen,<sup>a</sup> M. Duraffourg,<sup>a</sup> C. Vuitton,<sup>a</sup>  
S. Joffe,<sup>a</sup> C. Machado,<sup>a</sup> U. Fantz,<sup>b</sup> S. Mochalsky,<sup>b</sup> D. Wunderlich,<sup>b</sup> M. Lindqvist,<sup>b</sup>  
N. den Harder,<sup>b</sup> S. Briefi,<sup>b</sup> A. Hurlbatt,<sup>b</sup> T. Kalvas,<sup>c</sup> T. Minea<sup>d</sup> and A. Revel<sup>d</sup>

<sup>a</sup>CERN,

*Esplanade des Particules 1, P.O. Box, 1211 Geneva 23, Switzerland*

<sup>b</sup>Max-Planck-Institut für Plasmaphysik,

*Boltzmannstr. 2, D-85748 Garching, Germany*

<sup>c</sup>Department of Physics, University of Jyväskylä,

*P.O. Box 35 (YFL), 40014 Jyväskylä, Finland*

<sup>d</sup>Laboratoire de Physique des Gaz et des Plasmas, UMR 8578 CNRS, Université Paris-Saclay,

*Bat. 210, rue Henri Becquerel, 91405 Orsay, France*

*E-mail:* [Jacques.lettry@cern.ch](mailto:Jacques.lettry@cern.ch)

Abstract: A caesiated RF driven source delivers H<sup>-</sup> ions that, after stripping at the end of the 160 MeV H<sup>-</sup> linear injector, provides protons to CERN's accelerator complex including LHC, where the protons reached a record energy of 6.8 TeV. In Caesiated RF sources, H<sup>-</sup> ions are produced via dissociative attachment of electrons onto roto-vibrationally excited H<sub>2</sub>-molecules (volume) and re-emission as negative ions of protons or hydrogen atoms colliding on a low work function caesiated molybdenum plasma electrode (surface). During initial caesiation, the production mechanism evolves from the initial Cs-free volume production to a predominant surface production mode; the observed stunning reduction of co-extracted electrons is concomitant to an increase of the H<sup>-</sup> ion current to RF-power yield. This paper describes the evolution of the beam-profile at today's operational beam intensities of 35 mA for various ratios of volume and surface ion-origin. The presence of surface produced ions occurring on a conical plane is characterized by the electron to ion ratio and by measurement of the Cs-coverage of the molybdenum plasma electrode down to a fraction of a monolayer. Angular distributions are extracted from beam profile and Beam Emission Spectroscopy

---

\*Corresponding author.

(BES) measurements. These experimental results provide an initial comparison to beam formation simulation that, at a later stage, could be coupled to beam transport software packages.

The paper focuses on the caesiation transient to present experimental evidence for 3D beam formation studies, it provides insight into the mixing of volume and surface production modes, reduction of co-extracted electrons and Cs-coverage. The paper also establishes magnetic field induced asymmetries in the beam's current density.

Keywords: Ion sources (positive ions, negative ions, electron cyclotron resonance (ECR), electron beam (EBIS)); Accelerator Applications

---

## Contents

<b>1</b>	<b>Introduction</b>	<b>1</b>
<b>2</b>	<b>H<sup>-</sup> beam production modes</b>	<b>2</b>
<b>3</b>	<b>Electron to H<sup>-</sup> ion ratio and beam properties</b>	<b>3</b>
<b>4</b>	<b>Beam Emission Spectroscopy</b>	<b>6</b>
<b>5</b>	<b>Conclusion outlook</b>	<b>6</b>

---

## 1 Introduction

H<sup>-</sup> ion sources for accelerators require utmost stability and availabilities above 99%, these criteria are achieved by radio frequency (RF)-sources operated at the Oak Ridge Spallation Neutron Source (SNS), Tokai's Japan Proton Accelerator Research Complex (J-PARC), Dalang's China Spallation Neutron Source (CSNS) and the '*Conseil Européen pour la Recherche Nucléaire*' (CERN) [1]. The RF-class encompasses H<sup>-</sup> sources driven by inductively coupled RF plasma heating, equipped with a filter field separating the plasma heating and the low electron energy beam formation region and, usually, operated with a low work function caesiated plasma electrode.

RF-sources beam formation relies on two mechanisms: volume production described by Bacal [2, 3] is the result of a dissociative attachment of low energy electrons onto roto-vibrationally excited H<sub>2</sub>-molecules. Surface production was discovered at the Budker institute [4] and initially operated in Magnetron and Penning discharge sources successfully operated at the Brookhaven National Laboratory (BNL) and Rutherford Appleton Laboratory (RAL). Surface production consist in re-emission as H<sup>-</sup> ions of protons or hydrogen atoms impacting onto a low work function surface. In RF-sources, the low work function is obtained by deposition of a thin layer (few atomic monolayers) of Caesium on the inner surface of a metal electrode [5]. This so-called plasma electrode (PE) is located between the plasma and the extraction field regions. H<sup>-</sup> ions and electrons are extracted from the plasma meniscus through the plasma electrode aperture to form the H<sup>-</sup> and co-extracted electron beams. The meniscus is the surface separating the quasi-neutral plasma from purely negative ions and electrons beams, it is shaped by the plasma and extraction field that attracts negative and repels positively charged ions or molecular ions.

In caesiated RF-sources, beam formation combines volume ions with surface ions produced in a truncated conical surface around the plasma electrode aperture, it is at the crossing of plasma, surface, and beam physics. Magnetic field induced asymmetry requires 3D analysis, Orsay Negative Ion eXtraction (ONIX) [6] simulations of CERN's H<sup>-</sup> source are presented in ref. [7]. Beam formation is usually simulated via Monte Carlo Particle in Cell software packages [1, 8, 9]. Experimental validation encompasses Optical and Beam Emission Spectroscopy (OES, BES), Cs-coverage, profile

and emittance measurement, each requiring a dedicated setup [10]. As volume production is a feature of the plasma, it cannot be separated from surface production. The plasma parameters close to the extraction could not be measured by OES. Unfortunately, this region is difficult to access and the setup’s light transmission from the driver plasma is of typically  $O(1\%)$  and makes it difficult to interpret the collected OES data. As of today, NINJA simulation and OES analysis [11–14] are used to assess the plasma parameters in the beam formation region of the IS03  $H^-$  source.

This contribution characterizes the beam angular distribution, and beam profile around the nominal operation point of the IS03b  $H^-$  source [15] operated at 35 mA beam intensity (0.6 ms duration and 0.83 Hz repetition rate). The conditioning, volume and caesiated surface operation parameters are correlated to the Cs-coverage measured on the Molybdenum plasma electrode (aperture diameter: 7.5 mm).

## 2 $H^-$ beam production modes

CERN’s  $H^-$  sources are operated without multicusp and under Cs-loss compensation mode [16]. Operation a new source without Caesium at nominal plasma density while monitoring the electron and  $H^-$  current on a dedicated source test stand, is the so-called “conditioning” phase; a period of typically two weeks is sufficient to reduce and stabilize the co-extracted electrons yield  $e/H$  (electron to  $H^-$  current) from 100 down to  $e/H = 20\text{--}25$  that characterizes a clean plasma chamber and corresponds to optimal volume production. The source is then caesiated at low Cs mass flow during a few days to a week. During this period the ratio of volume to surface production evolves until the co-extracted electrons current is reduced to approximately match the  $H^-$  current ( $e/H = 1$ ). Figure 1 illustrates the 35 mA operation characterized by the RF-efficiency ( $H^-$  current/RF-power delivered to the plasma chamber) and  $e/H$ . The space charge of the electron beam is equivalent to the one of a 42.85 (velocities ratio) times smaller  $H^-$  current.

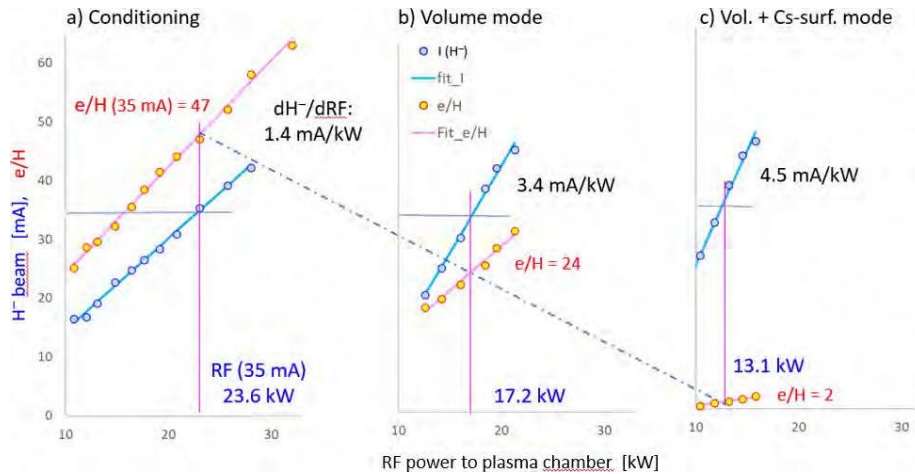


**Figure 1.** The electron yield and  $H^-$  current of the IS03 test unit. The values of the RF-power required to generate 35 mA  $H^-$  current and the corresponding electron yield are indicated for the conditioning (a), volume (b) and volume + surface (c) operation modes. The slope ( $dH^-/dRF$ ), RF power and  $e/H$  are indicated for 35 mA nominal  $H^-$  beam current.

Contribution of electrons to space charge ends when electrons are dumped which justifies reducing co-extracted electron and dumping shortly after extraction. The electron to ion ratio is the simplest and most reliable characterization of the source operation mode over its entire life cycle. By hypothetically postulating independence and simple linear addition in the contribution of volume and surface  $H^-$  ions to the resulting extracted beam, we could estimate that a 35 mA  $H^-$  beam extracted under  $e/H = 1$  and 13 kW RF to plasma is constituted of 42% vol. and 58% surf.  $H^-$  ions.

### 3 Electron to $H^-$ ion ratio and beam properties

The data were acquired at the source test stand, the electron current was measured on the source and beam dump power supplies,  $H^-$  current via a beam current transformer (BCT) and calibrated with a Faraday cup. Beam emittance and profile were acquired with a slit grid emittance meter. One plasma generator unit was cycled seven times with each time newly (ultra high vacuum bakeout) conditioned plasma electrodes. While beam data are accessible during operation, measurement of Cs-coverage requires removal of the plasma electrode and wet chemical sample preparation prior to X-ray fluorescence analysis [17]. Therefore, we interrupted operation at selected  $e/H$  values and associated Cs-coverage to the last recorded beam parameters, two plasma electrodes were operated in alternance to shorten the PE-replacement intervention time. The Cs-coverage on molybdenum substrate is approximated via the ratio of the Cs-mass per unit of surface (roughness neglected) to the density of metallic caesium, it is expressed in Cs-monolayer. During dismount and transport under atmosphere caesium that would have been in metallic form during operation will oxidize and wet chemistry sampling cannot distinguish between caesium or caesium oxide.

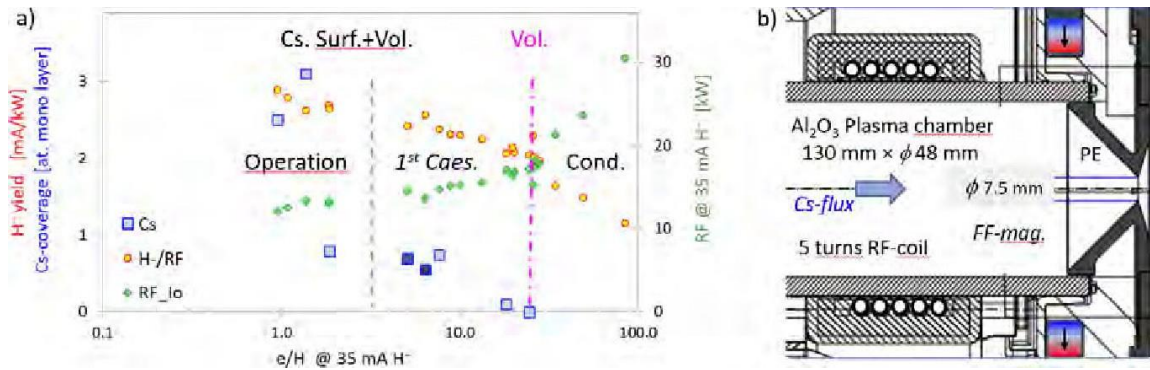


**Figure 2.** a) Source parameters: scatter plot of the RF-efficiency (circle), Cs coverage (square) and RF to plasma chamber (diamond) required to obtain a 35 mA  $H^-$  beam as a function of the electron to  $H^-$  ion ratio ( $e/H$ ). The plasma chamber conditioning (cond.), initial caesiation (noted 1<sup>st</sup> Caes.) and operation regions are indicated. The so-called volume mode (Vol.) after conditioning and prior to caesiation is indicated with a dash-dotted line, mixed volume and surface mode is noted Cs. Surf.+Vol. The Cs-coverage of two plasma electrodes ( $e/H$  of 5 and 6, dark squares) is the average value of three independently measured sectors. b) Layout of the plasma generator, plasma electrode and filter field magnets.

The  $e/H$ , RF power to plasma chamber (PRF) and RF-efficiencies ( $e_{RF} = H^-/PRF$ ) were interpolated to the 35 mA operation value from RF-power scans while the emittance and profile were recorded at beam intensities of 30 and 40 mA. Beam optics and high voltages were kept constant, RF

frequency and H<sub>2</sub> pulse parameters were slightly tuned whenever required. Figure 2 presents the Cs coverage (expressed in Cs-monolayer), the RF-efficiency and RF-power required to obtain a 35 mA H<sup>-</sup> beam as a function of e/H. The end of source conditioning is characterized by a change of slope of the PRF (35 mA) and H<sup>-</sup> yield; it corresponds to the so-called Volume mode of operation. For Linac4 H<sup>-</sup> Sources, the caesiation valve is opened once volume mode is reached. The RF power required to produce an H<sup>-</sup> beam is strongly correlated to e/H, beam production is most efficient at lowest e/H. At Linac4, the source is operated when e/H is below 4 and typically between 0.5 and 2, a RF regulation loop ensures stable current downstream the RFQ.

The data collected are representative of the transition towards the operation regime, it would be premature to conclude on an optimum Cs thickness for long term operation. For the last measurements corresponding to e/H of 5 and 6, the Cs-coverage sampling of plasma electrodes was split in three regions corresponding to successive ribbon-like layers of 6.5 mm of the plasma electrode inner surface along the beam axis. Actually, in the beam formation region surrounded by the plasma electrode, the plasma density drops by few orders of magnitude and the Cs-coverage results presented in figure 3 indicate a coverage gradient, where the thinnest coverage faces the higher plasma density. During constant Cs-flux initial caesiation of the order of 10 mg/month, we systematically observe a local maximum of the H<sup>-</sup> yield while e/H keeps decreasing during few hours or even days depending on the Cs-flowrate. Aiming at maximum yield and lowest e/H deserved further investigation of the possibly localized electron suppression mechanism. The electron suppression mechanism is likely related to the presence of a potential well resulting from surface emission of H<sup>-</sup> ion predicted by ONIX simulations [2]. The order of magnitude of this potential well corresponds to the electron energies measured in the beam formation region with Langmuir gauges or simulated by NINJA [14]. As an illustration, the potential well simulated with ONIX covering the IS03 beam intensity range is presented in figure 3c, for a 35 mA beam, the potential well is of the order of -0.5 V. The H<sup>-</sup> current originating from the surface (noted H<sup>-</sup> surf) is driven by surface emission and the volume contribution (H<sup>-</sup> volume = H<sup>-</sup> total - H<sup>-</sup> surf) by plasma parameters.

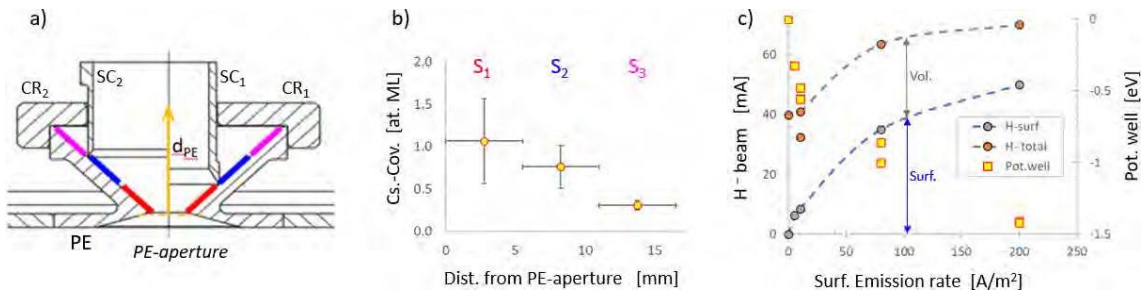


**Figure 3.** Cs-coverage sampling tools, each composed of a sampling cylinder (SC) and a centering ring (CR) and PE-geometry; the distance to plasma electrode aperture  $d_{PE}$  is indicated. b) Cs-coverage data (e/H of 5 and 6) as a function of  $d_{PE}$ . c) Potential well extracted from ONIX simulations [2] covering the IS03 operation range, assuming fixed plasma density and variable surface emission rate.

The slit-grid beam profile measurement is located after the first solenoid [18, 19] in the Low Energy Beam Transport (LEBT) section that matches the 45 keV beam to the Radio Frequency Quadrupole (RFQ) accelerator. The limited detection size imposes focusing the beam. We did not identify ways to correlate beam emittance to the dual volume and surface beam origin. However, the

beam profile radial distribution presented in figure 4 for 30 and 40 mA beam intensities shows a clear trend and drifts towards larger radii with decreasing  $e/H$  synonym of increasing  $H^-$  production on the PE-surface.

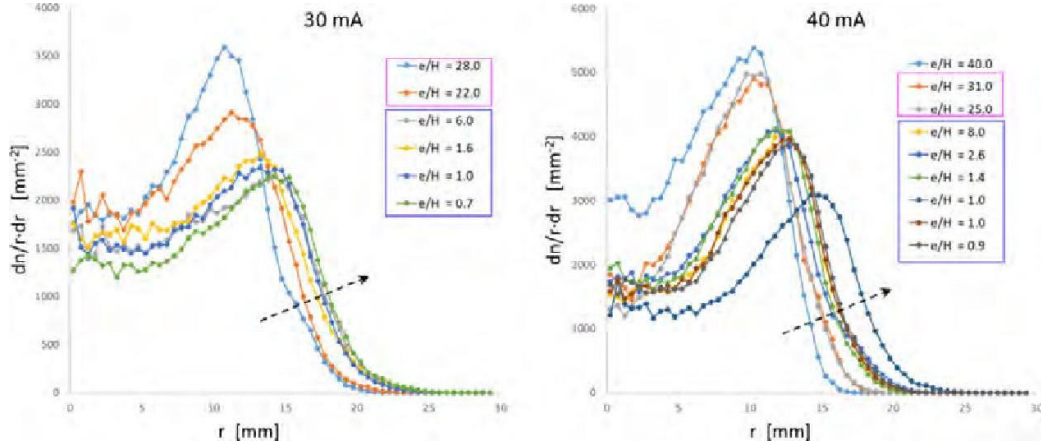


**Figure 4.** Radial beam profile  $dn/r-dr$  (Bining 0.25 mm) recorded in the LEBT after a solenoid at  $H^-$  beam intensities of 30 and 40 mA as a function of the electron to  $H^-$  ion ratio ( $e/H$ ). The beam broadening trend for smaller co-extracted electron yield is indicated with a dashed arrow.

Angular distributions of 30 and 40 mA beam derived from beam profile measurements are presented in figure 5. For volume and caesiated operation modes a clear angular dependence is observed and a factor of up to 2 is noted between minimum and maximum of the distribution. Top-down and left-right asymmetries are simple ratio of the beam contained in adjacent  $\pi/2$  sectors normalized to the average intensity. Their evolution as a function of the co-extracted electron yield ( $e/H$ ) for 30 and 40 mA beam intensities shows a larger asymmetry for low  $e/H$  that corresponds to a larger fraction of  $H^-$  ion surface production.

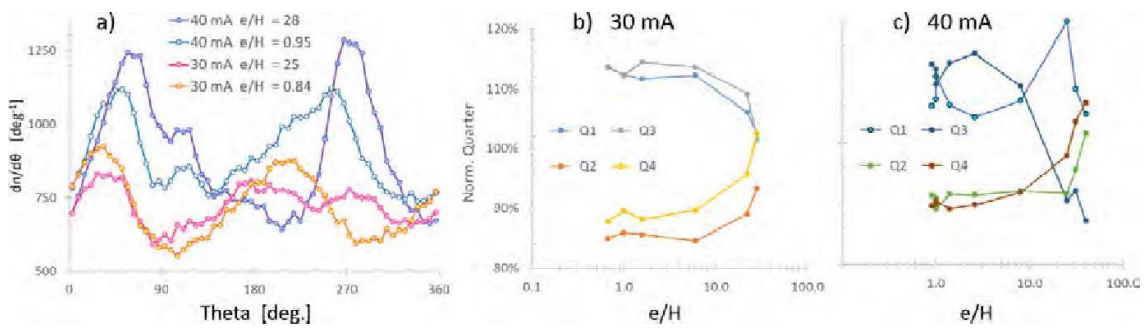


**Figure 5.**  $H^-$  beam angular distributions extracted from beam profile data for volume and caesiated operation mode characterized by high and low  $e/H$  ratios (a). The evolution of the integral over  $\pi/2$  quarter (normalized to the average of the 4 quarters) as a function of the co-extracted electron yield ( $e/H$ ) is presented for 30 (b) and 40 (c) mA  $H^-$  beam intensities.

## 4 Beam Emission Spectroscopy

In order to characterize the beam angular distribution via Beam Emission Spectroscopy, a telescope [20] is installed on two view ports located at 37 cm from the ion source, at a  $65^\circ$  angle to beam axis, the light emitted in a 12 mm diameter cylinder is collected onto a fiber and analyzed with a 2400 grating/mm spectrometer. The setup collects Doppler blue-shifted  $H_\alpha$  light emitted by H-atoms issued from neutralization of a fraction of the 45 keV  $H^-$  ion beam passing through a hydrogen gas pressure of 20 mPa.

BES spectra acquisition time was 10 hours corresponding to 20 s of effective beam duration, the beam intensity was approximately 50 mA, the RF-power to plasma 20 kW and  $e/H \approx 2-3$ . The angular dependance of the Doppler shift allows reconstruction of the beam angular distribution presented in figure 6. The analysis of the angular distribution provides a profile averaged across a cylinder of 6 mm radius centered on the beam axis. The beam profile extracted from BES data are corrected for local telescope capture efficiency under the simplifying assumption of a point like source. BES measurements after filter- and e-dump-fields show a  $\pm 12\%$  asymmetry in the horizontal plane and  $\pm 1\%$  in the vertical plane. The expected e-dump effect is a simple deflection that is corrected by a corresponding horizontal tilt of the source- to the beam-axis.

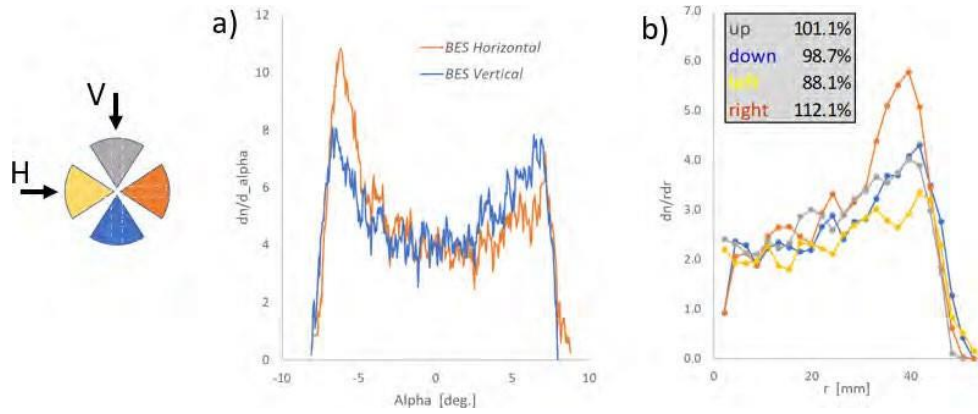


**Figure 6.** Distribution of the angle to beam axis a) extracted from BES spectra of the doppler shifted  $H_\alpha$  line along horizontal and vertical directions perpendicular to beam axis. Radial density distribution of the beam for each quadrant b), the BES acquisition regions and quadrants perpendicular to beam axis are indicated.

## 5 Conclusion outlook

This contribution presents experimental aspects of a collaborative effort that originally aimed at characterization of the inductively heated plasma (NIJNJA simulation and OES validation), beam formation via ONIX and beam transport (pending) to BES and emittance/profile measurement locations and eventually direct comparison of the transported beams to the experimental results. Parametrization via electron to ion ratio illustrates the various beam modes from conditioning to caesiated operation. The correlation between Cs-coverage averaged over the PE surface and beam parameters shows that 1–3 monolayer of Cs is suitable to start operation. However, we also established a non-uniformity of the plasma electrode Cs-coverage, understanding this anisotropy



deserves further work to improve plasma electrodes design for high  $H^-$  yield and low  $e/H$ . The test duration of few days and few mg Cs injection per data point do not exclude that thicker coverage provide suitable operation conditions, the sources operated in 2020–21 and 2022 and 60–65 mg Cs resulted in 20 respectively 100 ML homogeneously distributed on the plasma electrode surfaces and  $e/H$  ratio of 4 resp. 0.6 at the end of operation.

Beam profile distribution at constant  $H^-$  beam currents of 30 and 40 mA show a continuous morphing of the radial profile towards larger radii for increasing fraction of surface- to volume- $H^-$  ion origin.

The angular distribution of the beam measured in the LEBT is very asymmetric with a factor close to 2 between minimum and maximum; however, a trend of adjacent  $\pi/2$  sectors asymmetry is correlated to the co-extracted electron yield and is larger for lowest  $e/H$ . Beam formation and transport via ONIX coupled to IBSimu [21] simulation to the location of beam diagnostics is mandatory to disentangle contributions from the beam-formation- or beam-transport-origin to the non-gaussian (to say the least) beam profile angular and radial distributions. ONIX simulation [2] predicts a filter field induced beam asymmetry perpendicular to magnetic dipole axis; detailed BES measurements confirm a  $\pm 12\%$  effect in the horizontal plane and  $\pm 1\%$  in the vertical plane.

## References

- [1] M. Bacal ed., *Physics and Applications of Hydrogen Negative Ion Sources*, Springer-Nature (2023).
- [2] M. Bacal, A. Bruneteau, H. Doucet and W. Grahm,  *$H^-$  and  $D^-$  Production in plasma*, BNL Report-51304 (1980), p. 95.
- [3] M. Bacal and M. Wada, *Negative hydrogen ion production mechanisms*, *Appl. Phys. Rev.* **2** (2015) 021305.
- [4] Y.I. Belchenko, G.I. Dimov, V.G. Dudnikov and A.A. Ivanov, *On the formation of negative ions in gas discharge*, *Dokl. Akad. Nauk SSSR* **213** (1973) 1283.
- [5] W.G. Grahm, *Properties of Alkali Metals Absorbed onto Metal Surfaces*, in *Proc. on the 2nd Int. Symposium on the Production and Neutralization of Negative Ions and Beams*, Brookhaven National Laboratory, New York (1980), p. 126.
- [6] S. Mochalsky, A. Lifschitz and T. Minea, *3d modelling of negative ion extraction from a negative ion source*, *Nucl. Fusion* **50** (2010) 105011.
- [7] A. Vnuchenko et al., *Beam formation simulation of CERN's  $H^-$  caesiated RF source*, in proceedings of *8th International Symposium on Negative Ions, Beams and Sources*, Orto Botanico, Padova, Italy, 2–7 October 2022.
- [8] K. Miyamoto et al., *Numerical analysis of negative hydrogen ion beam optics by using 3D3V PIC simulation*, *AIP Conf. Proc.* **2011** (2018) 050012.
- [9] A. Revel, S. Mochalsky, I.M. Montellano, D. Wunderlich, U. Fantz and T. Minea, *Massive parallel 3d PIC simulation of negative ion extraction*, *J. Appl. Phys.* **122** (2017) 103302.
- [10] J. Lettry et al., *Beam Formation Studies on the CERN IS03b  $H^-$  Source*, *J. Phys. Conf. Ser.* **2244** (2022) 012036.
- [11] S. Mattei et al., *A fully-implicit Particle-In-Cell Monte Carlo Collision code for the simulation of inductively coupled plasmas*, *J. Comput. Phys.* **350** (2017) 891.

- [12] S. Mattei et al., *Numerical simulation of the RF plasma discharge in the Linac4  $H^-$  ion source*, *AIP Conf. Proc.* **1869** (2017) 030018.
- [13] S. Briefi et al., *Determination of discharge parameters via OES at the Linac4  $H^-$  ion source*, *Rev. Sci. Instrum.* **87** (2016) 02B104.
- [14] S. Briefi, S. Mattei, J. Lettry and U. Fantz, *Influence of the cusp field on the plasma parameters of the Linac4  $H^-$  ion source*, *AIP Conf. Proc.* **1869** (2017) 030016.
- [15] J. Lettry et al., *CERN's Linac4 cesiated surface  $H^-$  source*, *AIP Conf. Proc.* **1869** (2017) 030002.
- [16] J. Lettry et al., *Linac4  $H^-$  source R&D: Cusp free ICP and magnetron discharge*, *AIP Conf. Proc.* **2052** (2018) 050008.
- [17] J. Ory, C. Charvet and B. Teissandier, *Mesure de trace de Césium par XRF sur des surfaces métalliques pour le LINAC4*, <https://edms.cern.ch/document/2469324/1>, <https://edms.cern.ch/document/1555439/2>.
- [18] D. Noll et al., *Linac4 source extraction and low energy beam transport study*, *AIP Conf. Proc.* **2011** (2018) 080026.
- [19] B. Cheymol, *Development of beam transverse prole and emittance monitors for the CERN LINAC4*, Ph.D. thesis, Clermont-Ferrand U. (2011) [[CERN-THESIS-2011-289](#)].
- [20] A. Hurlbatt, *Unintuitive behaviour of fibre coupled collimating optics used for plasma emission observations*, *J. Phys. D* **53** (2020) 125204.
- [21] T. Kalvas, O. Tarvainen, T. Ropponen, O. Steczkiewicz, J. Ärje and H. Clark, *IBSIMU: A three-dimensional simulation software for charged particle optics*, *Rev. Sci. Instrum.* **81** (2010) 02B703.